Modeling and Stress Analysis of Doubly-Fed Induction Generator during Grid Voltage Swell

Zhou, Dao; Song, Yipeng; Blaabjerg, Frede

Published in:
Proceedings of the 42nd Annual Conference of IEEE Industrial Electronics Society, IECON 2016

DOI (link to publication from Publisher):
10.1109/IECON.2016.7793356

Publication date:
2016

Document Version
Accepted author manuscript, peer reviewed version

Modeling and Stress Analysis of Doubly-Fed Induction Generator during Grid Voltage Swell

Dao Zhou, Yipeng Song, Frede Blaabjerg

Department of Energy Technology
Aalborg University
Pontoppidanstraede 101, Aalborg, DK-9220, Denmark
zda@et.aau.dk, yis@et.aau.dk, fbl@et.aau.dk

***Abstract* - The Doubly-Fed Induction Generator (DFIG) based wind turbine system is presently dominant in the wind turbine market. Due to heavy load switch-off and faults in the power grid, voltage swells may occur and this phenomenon is currently given sufficient insights. This paper starts to describe the DFIG modeling and challenges when facing the symmetrical voltage swell. Then, the High Voltage Ride-Through (HVRT) capability of the DFIG can be calculated by using the demagnetizing current control, and the stator current, rotor current as well as the electromagnetic toque can be deduced during the transient voltage swell and its recovery. It is concluded that although both higher swell level and higher rotor speed cause higher rotor electromotive force, the doubly-fed induction generator can successfully ride through the grid fault due to the relatively small swell level required by the modern grid codes. Additionally, the calculated maximum stresses of the DFIG can be verified by simulation results in terms of the rotor current, stator current, and the toque at various swell levels.**

I. INTRODUCTION

The effects of voltage dip on wind turbine and control strategies of the Low Voltage Ride-Through (LVRT) have been extensively studied [1]-[7]. However, voltage swells may occur due to the large load and capacitor bank switch-off or the faults in the grid, and this phenomenon is currently given sufficient insights. Although the High Voltage Ride-Through (HVRT) requirement is not as much discussed as the modern LVRT specifications, the HVRT capabilities are expected to gradually become mandatory with the increasing capacity of the wind power [8]-[10]. Fig. 1 shows the Australia formulated HVRT guidelines for wind turbines [8], and it stipulates that the wind turbine should be able to withstand 1.3 pu grid voltage for maximum 60 ms. Besides, in the case of the voltage swell is less than 0.1 pu, the wind turbine system should stay connected for a long term, basically all the time.

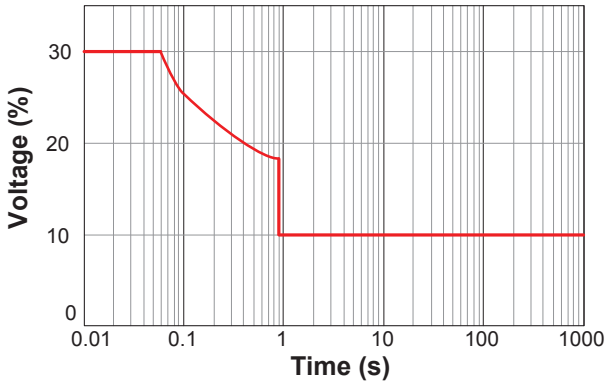

Fig. 1. High voltage ride-through requirement stated in Australian grid codes.

The Doubly-Fed Induction Generator (DFIG) based wind turbine system is presently dominant in the wind turbine market. Since the stator of the induction generator is directly linked to the power grid, a natural stator flux is inevitably introduced in the case of the stator voltage change, which may induce over-voltage and over-current issues of the Rotor-Side Converter (RSC). The state-of-the-art fault ride-through approaches consist of hardware and software solutions [3]-[7]. In respect to hardware solutions, as shown in Fig. 2, the Dynamic Voltage Restorer (DVR) can maintain a constant stator voltage, and can avoid the occurrence of the natural stator flux [3]. On the other hand, the rotor-side crowbar or dc-side chopper can be used to accelerate the damping of the natural stator flux and prevent the fragile power electronic devices from over-voltage and over-current [4], [5]. A software solution like the demagnetizing current control is also promising due to its cost-effectiveness [6], [7], but the extent of this application is closely related to the power rating of the RSC, and it becomes challenging during the serious voltage dips. As most of solutions are applied in the case of the LVRT, their realization during the HVRT is seldom discussed. This paper focuses on the feasibility of the demagnetizing current control facing the grid voltage swell, and the modeling and transient stress of the DFIG current and the electromagnetic torque are quantitatively analyzed.

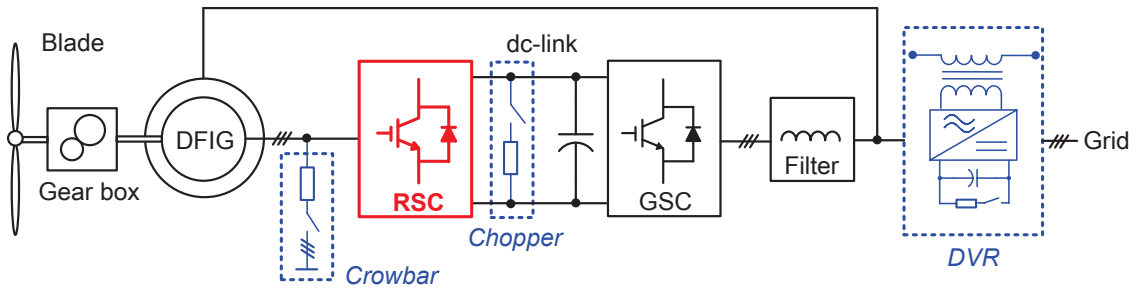

Fig. 2. State-of-the-art solutions for doubly-fed induction generator to ride through grid faults (GSC: Grid-Side Converter; RSC: Rotor-Side Converter; DVR: Dynamic Voltage Restorer).

The remaining part of this paper is organized as follows. Section II describes the modeling and challenges in the DFIG when it is subject to the grid voltage swell. By using a demagnetizing current control strategy, section III starts with a capability analysis of the DFIG facing the HVRT, and then calculates the transient rotor current, stator current and torque of the DFIG. Afterwards, the expected calculations are verified by simulations in terms of the maximum stress on the DFIG in section IV. Finally, some concluding remarks are drawn in last section.

II. DFIG Modeling and Challenges Subject to Grid Voltage Swell

As shown in Fig. 2, a voltage swell in the power grid affects the performances of both the Grid-Side Converter (GSC) and the RSC. Normally, the dc-link voltage has a small margin of the modulation index for lower switching loss of the power semiconductors, so over modulation of the dc-link is most important challenge for the GSC. A flexible dc-link voltage with the increasing amplitude of the grid voltage is proposed, and tried in order to keep the controllability of the GSC [11]. As a consequence, this paper mainly addresses the challenges seen from the RSC.

In the case of the symmetrical voltage swell, the equivalent circuits of the DFIG are depicted in Fig. 3. Due to the lack of the negative component, the modeling of the DFIG can be divided into the natural machine and the forced machine, which separately represent the transient components and the steady-state component. It is noted that under the stator reference frame, the components of the natural machine become dc due to the exponentially decreasing natural stator flux, while the components of the forced machine is still ac caused by the swelled grid voltage, which has the same frequency as the stator-side.

A dc component in respect to the stator reference frame rotates at the frequency of the rotor speed ω_r, while the component at the stator frequency ω_1 rotates at the frequency of the slip speed ω_s under the rotor reference frame. Besides, the rotor voltage is approximately the differential of the rotor flux in the rotor reference frame. Due to the fact that the rotor frequency is normally 5-8 times higher than the slip frequency, the natural rotor voltage, which is proportional to the rotor

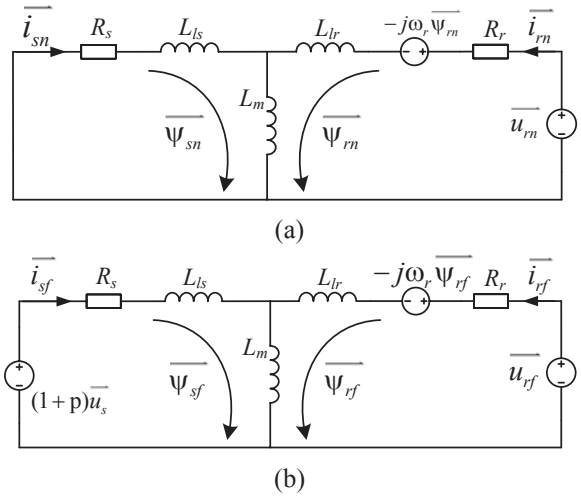

Fig. 3. Equivalent circuits of DFIG during a symmetrical voltage swell. (a) Natural machine model stands for transient components; (b) Forced machine model stands for steady-state components.

speed, becomes considerably higher compared to the forced rotor voltage, related to the slip speed. As a consequence, an over-voltage problem can be expected, which further causes an over-current because the RSC is out of control. On the other hand, during the transient period, the electromagnetic torque may suffer from the fluctuations because of the irregular DFIG stator and rotor current, which gives an additional mechanical stress of the gearbox. It challenges reliable operation of the gearbox, which has the longest downtime among the components of the wind turbine system [12].

III. Stress Analysis of DFIG during Transient Period

With the advantage that the capacity of the rotor current is fully contributing to the fastest decaying of the natural flux and mitigation of the high rotor voltage, the demagnetizing current control is a widely used method during the fault ride-through [6]. As shown in Fig. 4, its control objective switches to the opposite direction of the natural stator flux ψ_{sn} from the stator active power P_s and reactive power Q_s. Compared to the vector control in normal operation, a process of the stator flux observation and extraction is required additionally.

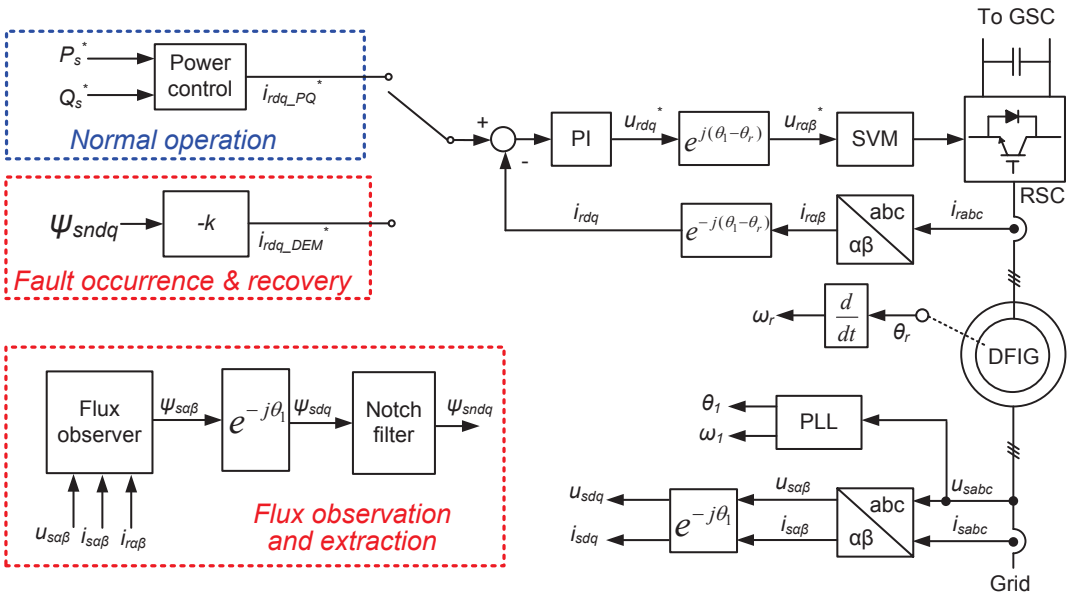

Fig. 4. Control schemes of rotor-side converter in normal operation and voltage swell period.

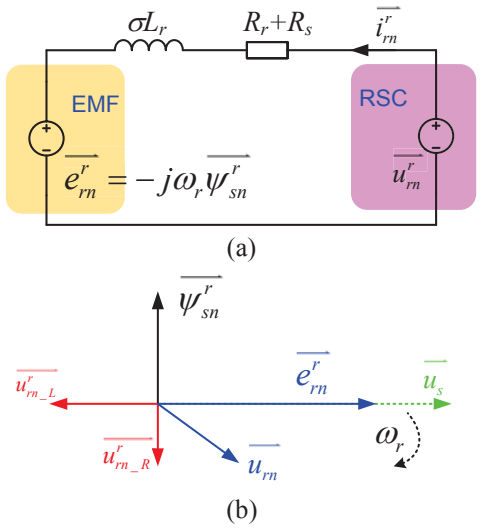

Fig. 5. Relationship between rotor voltage and rotor current viewed from the rotor-side. (a) Equivalent circuit; (b) Space vector diagram.

As aforementioned, since the component of the natural rotor voltage is much higher than the forced rotor voltage, only the natural machine model is taken into account when considering the HVRT capability of the DFIG. On the basis of the voltage and flux equations as shown in Fig. 3(a), the relationship between the natural rotor voltage u_{rn} and the natural rotor current i_{rn} in the rotor reference frame can be expressed as [6],

$$\overrightarrow{u_{rn}^r} \approx \underbrace{(R_r + R_s)\overrightarrow{i_{rn}^r}}_{\overrightarrow{u_{rn\_R}^r}} + \underbrace{\sigma L_r \frac{d}{dt}\overrightarrow{i_{rn}^r}}_{\overrightarrow{u_{rn\_L}^r}} + \underbrace{(-j\omega_r \overrightarrow{\psi_{sn}^r})}_{\overrightarrow{e_{rn}^r}} \tag{1}$$

Table I
SPECIFICATION OF 2 MW DOUBLY-FED INDUCTION GENERATOR AND ITS ROTOR-SIDE CONVERTER.

Doubly-fed induction generator	
Rated power	2 MW
Operational range of rotor speed	1050-1800 rpm
Rated amplitude of stator phase voltage	563 V
Rated frequency	50 Hz
Rated amplitude of stator phase current	2368 A
Rated electromagnetic torque	12.7 kNm
Stator resistance	1.69 mΩ
Rotor resistance	1.52 mΩ
Mutual inductance	2.91 mH
Stator leakage inductance	0.04 mH
Rotor leakage inductance	0.06 mH
Ratio of stator winding and rotor winding	0.369
Rotor-side converter	
Rated power	400 kW
Rated amplitude of rotor phase current	915 A
Rated amplitude of rotor phase voltage	305 V
DC-link capacitor	20 mF
DC-link voltage V_{dc}	1350 V
Switching frequency f_{sw}	2 kHz
Used power module in each arm	1 kA/1.7 kV; two in parallel

where R_s, R_r and L_r denote the stator resistance, the rotor resistance and inductance, σ denotes the leakage coefficient. It is noted that the rotor voltage is largely determined by the

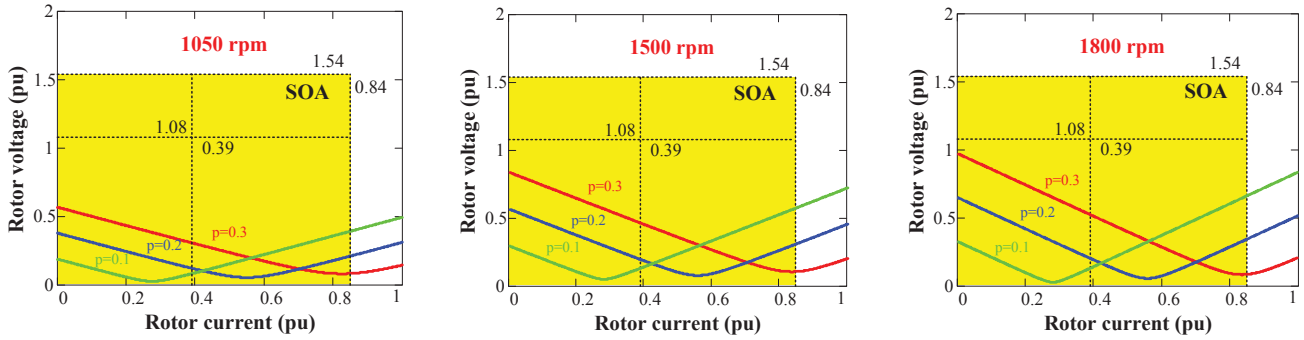

Fig. 6. Voltage swell level effect on HVRT capability of the DFIG at various rotor speeds. (a) 1050 rpm; (b) 1500 rpm; (c) 1800 rpm.

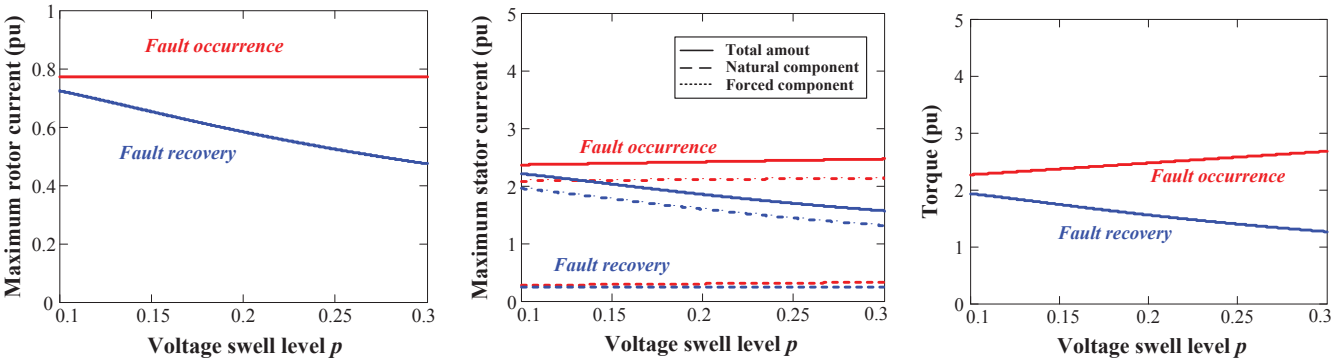

Fig. 7. Stress analysis of the DFIG at different levels of voltage swell and recovery. (a) Maximum rotor current; (b) Maximum stator current; (c) Maximum torque.

ElectroMotive Force (EMF) e_{rn}, which is the product of the natural stator flux ψ_{sn} and the rotor frequency, as the voltage drop across the rotor resistor u_{r_R} and the transient rotor inductor u_{r_L} are normally small enough.

The equivalent circuit of the DFIG seen from the rotor-side is shown in Fig. 5(a), and its space vector diagram is depicted in Fig. 5(b). It can be seen that during the voltage swell, the natural stator flux leads the stator voltage 90 degree, and the EMF keeps the same direction as the stator voltage. If the rotor current is regulated in the opposite direction of the natural stator flux, the voltage drop across the transient rotor inductor is able to counteract the EMF.

With the specifications of a 2 MW DFIG, its RSC and the power devices used in the RSC as listed in Table I, the Safe Operation Area (SOA) of the RSC can be expected. It is noted that the RSC can withstand up to 0.84 pu base current and 1.54 base voltage, while the rotor current and rotor voltage only consume 0.39 pu and 1.08 pu base value at the rated power.

As listed in (1), the rotor EMF is closely related to the rotor speed and the natural stator flux, which is proportional to the swell level p. The HVRT capability of the RSC can be analyzed at various rotor speeds and swell levels in [6], where the rotor speeds of 1050 rpm, 1500 rpm and 1800 rpm are selected to represent the sub-synchronous, synchronous, and super-synchronous operation, and swell level is up to 0.3 according to the grid codes. It can be seen that both the higher rotor speed and the higher swell level cause a higher rotor voltage. Moreover, it is evident that the DFIG can successfully ride through all swell levels at different rotor speeds. In order to accelerate the damping of the natural stator flux, a 0.75 pu demagnetizing rotor current is selected. Besides, as the rotor speed of 1800 rpm has the highest EMF, this situation will be further in focus in terms of the transient rotor current, stator current and torque. Since the recovery from the swelled voltage also introduces the natural component of the stator flux, the demagnetizing current is injected again for a certain period before the normal vector control is applied. In this study, the fault period is assumed 60 ms according to the Australian grid code, and the demagnetizing control is applied for 50 ms after the fault clearance.

As a fixed 0.75 pu rotor current is controlled in the opposite direction of the natural stator flux, there is no forced component of the rotor current. However, the stator current not only contains the natural component related to the natural

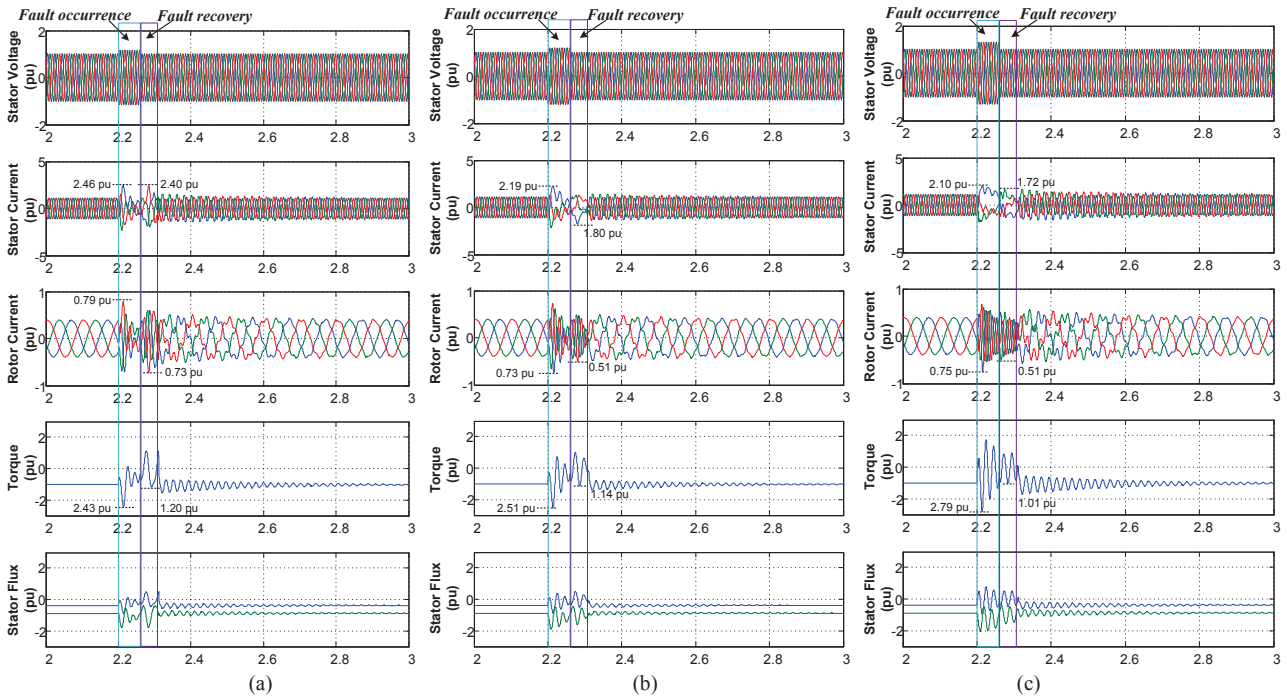

Fig. 8. Simulation results of DFIG operation at 1800 rpm with various levels of voltage swell and recovery. (a) Swell level of 0.15; (b) Swell level of 0.2; (c) Swell level of 0.3.

rotor current, but also includes the forced stator current generated by the excitation energy of the induction generator by the swelled grid voltage. Furthermore, as the electromagnetic torque is related to the stator current and the rotor current, the transient torque can be deduced [7]. As a consequence, the maximum rotor current, stator current and torque are calculated and they are shown in Fig. 7. In the case of a fault occurrence, it can be seen that the stator current and torque increases with the higher swell level in despite of the constant rotor current. In the case of the fault recovery, as the natural stator flux caused by the voltage swell is counteracted by the natural stator flux introduced by the fault clearance at the instant of 60 ms, it can be observed that the maximum rotor current decreases with higher swell level. Similarly, the maximum stator current and torque also decreases with higher swell level.

IV. Simulation Validation

In this section, the theoretical stress analysis of the DFIG during the period of the voltage swell is verified by using Matlab Simulink. The parameters of the 2 MW system are consistent with Table I. A 60 ms fault occurs at the instant of 2.2 second, and the demagnetizing current control is applied during the fault period and within 50 ms after the fault clearance. As shown in Fig. 8, the stator current, rotor current, torque and the stator flux are simulated at the swell levels of 0.15, 0.2 and 0.3, respectively.

During the fault occurrence and fault recovery, the maximum values of the stator current, rotor current and the torque are marked and compared with the calculated values as

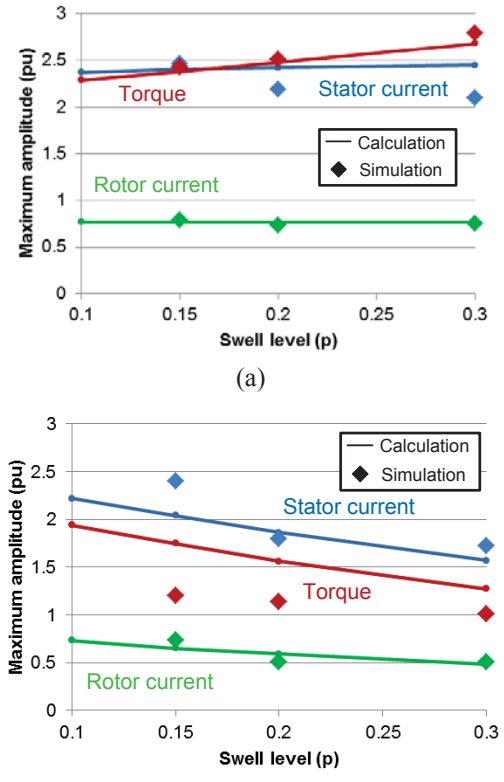

Fig. 9. Calculation and simulation of the maximum stator current, rotor current and torque of DFIG during (a) voltage swell, and (b) voltage recovery.

shown in Fig. 9. Due to the time delay and phase shift introduced by the notch filter as well as the instant tracking error of the PI controller for a low ac component, there is a small discrepancy between the theory and simulation, especially for the torque and the stator current. However, it can be clearly seen that the tendency of the simulation results well matches the calculation. For instance, in the case of a voltage swell, a constant 0.75 pu demagnetizing rotor current causes a 2.46 pu, 2.19 pu and 2.10 pu maximum stator current, and a 2.43 pu, 2.51 pu and 2.79 pu maximum torque in the swell levels of 0.15, 0.2, and 0.3, respectively. However, the demagnetizing rotor current becomes 0.73 pu, 0.51 pu, and 0.51 pu in the case of swell recovery, and the stator current and torque also decrease with the higher swell level.

V. CONCLUSION

This paper describes the modeling and challenges of the doubly-fed induction generator facing the symmetrical voltage swell, and it gives an approach to theoretically calculate current and torque stress during this transient period by using the demagnetizing current control. It is concluded although both the higher swell level and the higher rotor speed causes higher rotor electromotive force, the doubly-fed induction generator can successfully ride through the fault due to the relatively small swell level required by the modern grid codes. Additionally, the calculated maximum stresses of the induction generator are able to be verified by the simulations in terms of the rotor current, the stator current and the electromagnetic torque.

References

[1] F. Blaabjerg, and K. Ma, "Future on power electronics for wind turbine systems," *IEEE Journal of Emerging and Selected Topics in Power Electronics*, vol. 1, no. 3, pp. 139-152, Sep. 2013.

[2] C. Huang, F. Li, and Z. Jin, "Maximum power point tracking strategy for large-scale wind generation systems considering wind turbine dynamics," *IEEE Trans. on Industrial Electronics*, vol. 62, no. 4, pp. 2530-2539, Apr. 2015.

[3] C. Wessels, F. Gebhardt, and F. W. Fuchs, "Fault ride-through of a DFIG wind turbine using a dynamic voltage restorer during symmetrical and asymmetrical grid faults," *IEEE Trans. on Power Electronics*, vol. 26, no. 3, pp. 807-815, Mar. 2011.

[4] J. Morren, and S. W. H. Haan, "Ridethrough of wind turbines with doubly-fed induction generator during a voltage dip," *IEEE Trans. on Energy Conversion*, vol. 20, no. 2, pp. 435-441, Jun. 2005.

[5] G. Pannell, B. Zahawi, D. J. Atkinson, and P. Missailidis, "Evaluation of the performance of a DC-link brake chopper as a DFIG low-voltage fault-ride-through device," *IEEE Trans. on Energy Conversion*, vol. 28, no. 3, pp. 535-542, Sep. 2013.

[6] J. Lopez, E. Gubia, E. Olea, J. Ruiz, and L. Marroyo, "Ride through of wind turbines with doubly fed induction generator under symmetrical voltage dips," *IEEE Trans. on Industrial Electronics*, vol. 56, no. 10, pp. 4246-4254, Oct. 2009.

[7] W. Chen, D. Xu, N. Zhu, M. Chen, and F. Blaabjerg, "Control of doubly-fed induction generator to ride-through recurring grid faults," *IEEE Trans. on Power Electronics*, vol. 31, no. 7, pp. 4831-4846, Jul. 2016.

[8] *Australian Energy Market Commission*, National electricity rules. (Available: http://www.aemc.gov.au.)

[9] E.ON-Netz. *Requirements for offshore grid connections*, Apr. 2008.

[10] Force, W. G. T. The technical basis for the new WECC voltage ride-through (VRT) standard, Jun. 2007.

[11] C. Liu, X. Huang, M. Chen, and D. Xu, "Flexible control of DC-link voltage for doubly fed induction generator during grid voltage swell," *in Proc. of ECCE 2010*, pp. 3091-3095, 2010.

[12] D. Zhou, F. Blaabjerg, M. Lau, and M. Tonnes, "Optimized reactive power flow of DFIG power converters for better reliability performance considering grid codes," *IEEE Trans. on Industrial Electronics*, vol. 62, no. 3, pp. 1552-1562, Mar. 2015.